Article

Preparation and Thermal Performance of Fatty Acid Binary Eutectic Mixture/Expanded Graphite Composites as Form-Stable Phase Change Materials for Thermal Energy Storage

Dongyi Zhou,* Shuaizhe Xiao, and Xianghua Xiao

Read Online

ACCESS | Metrics & More | Article Recommendations

ABSTRACT: A series of fatty acid binary eutectic mixture/expanded graphite (FABEM/EG) composite phase change materials (CPCMs) were prepared by absorbing a liquid FABEM into the EG. The thermal properties, thermostability, and thermoreliability were determined by differential scanning calorimetry (DSC), thermogravimetric analysis (TGA), and thermal cycling tests, respectively. Fourier transform infrared spectrometry (FT-IR) and scanning electron microscopy (SEM) were used to analyze the chemical structure and microstructure, respectively. Thermal conductivity measurements and heat storage/release experiments were carried out to study the heat transfer performance. The DSC test results show that the phase transition temperatures and latent heat of these CPCMs are in the range of 17.8−55.2 °C and 134.9−176.2 J/g, respectively. FT-IR analysis indicates there is only a simple physical adsorption between EG and the PCM and no chemical reaction occurs. SEM results show that the fatty acid binary eutectic mixtures are well adsorbed in the pores of EG, and EG can provide a certain mechanical strength and prevent phase change materials from leaking. The thermal conductivity measurement and heat storage/release experiment show that the addition of EG greatly improves the thermal conductivities of the CPCMs. TGA test results and thermal cycle tests show that the CPCMs have excellent thermal stability and long-term cycling thermal reliability.
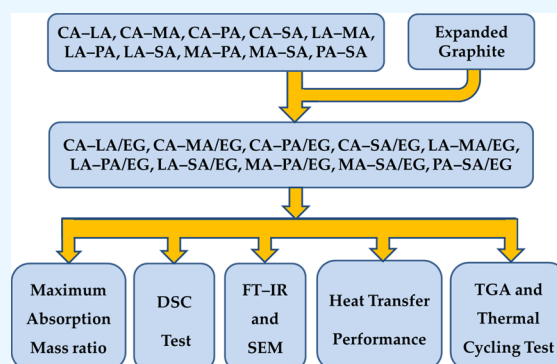
1. INTRODUCTION

Energy storage technology is one of the effective methods to solve the energy crisis, and it has broad application prospects in the fields of shifting peaks and valleys of power, solar energy utilization, industrial waste heat recycling, building heating, and air conditioning.[1−5] Thermal energy storage can generally be divided into chemical energy storage,[6−8] sensible heat storage,[9] and latent heat storage.[10,11] Latent heat storage has many advantages, including high energy storage density, low temperature change, excellent material stability, and high safety, so it has received a significant amount of attention and application.[12−16] Fatty acids have attracted much attention for their appropriate phase change temperature, high phase change latent heat, nontoxicity, noncorrosiveness, no or small volume change, small degree of subcooling, good thermal reliability, abundant raw materials, easily obtainable, and other advantages.[17,18] More importantly, two or more fatty acids can be mixed into a eutectic mixture according to the eutectic effect of fatty acids to reduce the phase change temperature and expand its temperature application range.[19,20] Although fatty acid eutectic mixtures have many advantages, they also have the disadvantages of poor thermal conductivity and easy leakage.[21−23] At present, the common method to solve these

problems is to add materials with high thermal conductivity and porous structures to fatty acid PCMs.[24−26] Due to its low density, high thermal conductivity, and porous structure, expanded graphite (EG) is frequently utilized as a substrate material, which not only minimizes liquid leakage but also significantly improves the thermal conductivity of the PCMs.[27−30]

Fei et al. prepared capric−palmitic acid/expanded graphite (CA−PA/EG) with the EG optimum mass content of 11.1%; the results confirmed that the addition of EG may enhance the heat conductivity together with boosting the heat storage/release speed of CA−PA, and the CA−PA/EG CPCM with the optimum mass ratio provides superior heat stableness and chemical stability.[31] Huang et al. prepared the pahnitic acid−stearic acid/bentonite/expanded graphite CPCMs with bentonite used as the supporting material and expanded

graphite used to prevent eutectic mixtures from leaking while also improving the thermal conductivity of the CPCMs, and the experimental results of heat storage/release show that the heat transfer of the CPCMs with EG is enhanced.[32] Sari prepared bentonite-based form-stable composite PCMs (Bb-FSPCMs) with an EG mass content of 5 wt % and found that the addition of EG enhanced the heat transfer performance.[33]

Most studies focus on a few fatty acid binary eutectic mixture/expanded graphite (FABEM/EG) CPCMs, and systematic theoretical research and experimental characterization have not been carried out. In this paper, on the basis of our previous research,[23,34,35] 10 FABEM/EG CPCMs were prepared by the physical adsorption method with fatty acid binary eutectic mixtures as PCMs and expanded graphite as the substrate material. The maximum absorption mass ratio (MaxAMR) of the FABEM in CPCMs is determined. The thermal properties, thermostability, and thermoreliability were determined by DSC, TGA, and thermal cycling tests, respectively. FT-IR and SEM were used to analyze the chemical structure and microstructure, respectively. A thermal conductivity measurement and heat storage/release experiment were carried out to study the heat transfer performance. The findings provided guidance for the application of FABEM/EG CPCMs.

2. MATERIALS AND METHODS

2.1. Materials. Capric acid (CA, analytically pure), lauric acid (LA, analytically pure), myristic acid (MA, analytically pure), palmitic acid (PA, analytically pure), and stearic acid (SA, analytically pure) were obtained from Shanghai Zhunyun Chemical Co, Ltd., China. Expandable graphite (350 meshes, 100 mL/g expansion coefficient, carbon content >99%) was purchased from Qingdao Hengrunda Graphite Products Co, Ltd., China.

2.2. Preparation of Fatty Acid Binary Eutectic Mixture/Expanded Graphite CPCMs. Expanded graphite is obtained by heating dry expandable graphite in a very ceramic crucible for 40 s in a 800 °C muffle furnace, and its pore diameter is 2−100 nm. Ten FABEM PCMs were prepared according to our previous studies, and the eutectic points are shown in Table 1.[36,37] Certain amounts of FABEM

Table 1. Eutectic Point of 10 Fatty Acid Binary Eutectic Mixtures

CPCMs	eutectic mass ratio	CPCMs	eutectic mass ratio
CA−LA	62.0/38.0	LA−PA	70.7/29.3
CA−MA	72.2/27.8	LA−SA	81.2/18.8
CA−PA	81.1/18.9	MA−PA	60.3/39.7
CA−SA	89.7/10.3	MA−SA	71.8/28.2
LA−MA	60.4/39.6	PA−SA	62.1/37.9

PCM and EG are placed inside the exact same beaker. Subsequent to blending the sample together consistently, the film-sealed beaker is positioned in a vacuum drying oven at a certain temperature for 48 h. To ensure that the FABEM PCM is uniformly adsorbed in the EG, it is stirred every 2 h. Then, the beaker was taken out of the vacuum drying oven and cooled to room temperature and the FABEM/EG CPCM was obtained.

2.3. Characterization. The phase transition temperature (melting and freezing temperature, T_m and T_f) and latent heat (melting and freezing latent heat, H_m and H_f) of FABEM

PCMs and FABEM/EG CPCMs were determined using a differential scanning calorimeter (DSC, NETSZCH 214Polyma, Germany). Samples between 5 and 10 mg were placed in an aluminum crucible and sealed. Then, the samples were scanned at a heating rate of 5 °C/min under a nitrogen atmosphere. The accuracy of phase change temperature and latent heat is ±0.1 and ±4%, respectively. The chemical structure of the material was analyzed using a Fourier transform infrared spectrometer (FT-IR, Thermo Scientific Nicolet iS10), which was operated from 400 to 4000 cm^{-1} with a resolution of 2 cm^{-1}, using KBr pellets. Scanning electron microscopy (SEM, Phenom LE, Phenom-World, The Netherlands) is used to observe the micromorphology of the FABEM/EG CPCMs.

The thermal conductivity of the samples was investigated using a thermal conductivity tester (DRE-III, Xiangtan Xiangyi Instrument and Instrument Co., Ltd., China). The sample is made into cakes with a smooth surface and different densities, and then, its thermal conductivity is obtained by the measurement. Heat storage and release experiments are carried out on the sample within a certain temperature range, and the temperature is recorded every 10 s.

The thermostability of the samples was studied using thermogravimetric analysis (TGA, TA TGA5000IR) with the CPCMs heated from 20 to 400 °C at a heating rate of 10 °C/min under a nitrogen atmosphere with an error of ±0.2%. The thermoreliability of the CPCM was determined by the thermal cycling test. After multiple thermal cycles, the DSC test was repeated again to detect the thermal properties of the recycled PCM.

3. RESULTS AND DISCUSSION

3.1. MaxAMR of Fatty Acid Binary Eutectic Mixtures in CPCMs. In general, the more the phase change material content in CPCMs, the greater the latent heat of the CPCMs. To make CPCMs contain more fatty acids without leakage, it is necessary to conduct experiments on the ratio of PCMs to EG and determine the MaxAMR of PCMs in CPCMs. According to the method of the percentage determination of penetration diameter in the literature,[38] we determined the MaxAMR of 10 fatty acid binary eutectic mixtures in FABEM/EG CPCMs, and the results are shown in Table 2. It can be seen that the MaxAMR of fatty acid binary eutectic mixtures in CPCMs is in the range of 92.0−93.2%.

Table 2. MaxAMR of Fatty Acid Binary Eutectic Mixtures in CPCMs

CPCMs	MaxAMR (%)	CPCMs	MaxAMR (%)
CA−LA/EG	92.0	LA−PA/EG	93.2
CA−MA/EG	92.2	LA−SA/EG	93.0
CA−PA/EG	92.4	MA−PA/EG	92.8
CA−SA/EG	92.2	MA−SA/EG	92.6
LA−MA/EG	92.2	PA−SA/EG	92.8

3.2. Thermal Properties of the CPCMs. The phase transition temperature and latent heat of CPCMs can be measured by DSC. The DSC curves of the 10 FABEM PCMs and FABEM/EG CPCMs are shown in Figure 1, and the phase transition parameters are shown in Table 3. The phase transition temperatures and latent heat of the FABEM/EG CPCMs are in the range of 17.8−55.2 °C and 134.9−176.2 J/g, respectively. The phase transition temperature of the PCM is
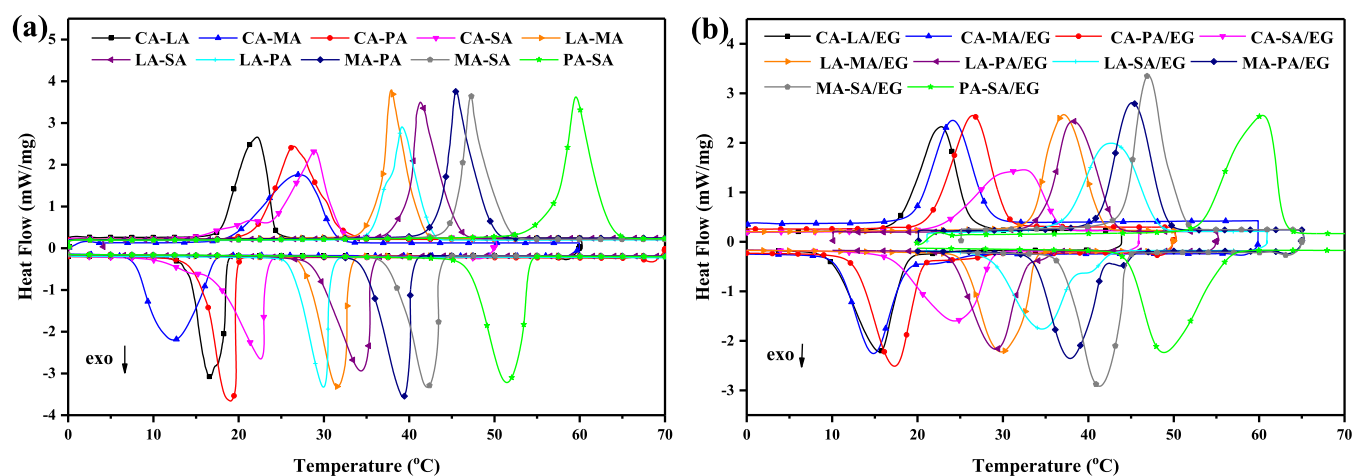
Figure 1. DSC curves of 10 fatty acid binary eutectic mixtures (a) and 10 FABEM/EG CPCMs (b).

Table 3. Thermal Performance Parameters of the 10 Fatty Acid Binary Eutectic Mixtures and 10 CPCMs

	melting		freezing	
PCMs/CPCMs	T_m (°C)	H_m (J/g)	T_f (°C)	H_f (J/g)
CA−LA	17.7	155.2	18.6	142.2
CA−LA/EG	17.8	142.5	18.7	141.0
CA−MA	19.4	150.9	18.4	149.2
CA−MA/EG	19.7	137.3	18.8	139.8
CA−PA	22.1	165.6	20.0	159.7
CA−PA/EG	21.5	151.7	20.7	149.5
CA−SA	23.4	150.5	23.4	148.0
CA−SA/EG	23.0	134.9	25.3	133.7
LA−MA	36.1	158.9	32.8	149.7
LA−MA/EG	33.3	153.9	33.9	144.3
LA−PA	37.8	164.0	34.6	154.8
LA−PA/EG	34.7	152.6	32.9	142.8
LA−SA	39.9	167.1	35.6	158.3
LA−SA/EG	37.2	158.7	38.8	143.3
MA−PA	44.1	182.2	40.4	171.9
MA−PA/EG	41.3	162.1	42.1	152.3
MA−SA	44.8	186.9	43.7	184.4
MA−SA/EG	44.1	174.2	44.6	171.9
PA−SA	57.1	193.0	53.7	188.6
PA−SA/EG	55.2	176.2	54.9	175.6

Table 4. Comparison of the Experimental and Calculated Values of H_m

CPCMs	PCM mass content in CPCM (x, %)	experimental value (kJ/kg)	calculated value (kJ/kg)	relative error (%)
CA−LA/EG	92.0	142.5	142.8	0.20
CA−MA/EG	92.2	137.3	139.1	1.33
CA−PA/EG	92.4	151.7	153.0	0.87
CA−SA/EG	92.2	134.9	138.8	2.86
LA−MA/EG	92.2	153.9	146.5	−4.80
LA−PA/EG	93.2	152.6	152.8	0.16
LA−SA/EG	93.0	158.7	155.4	−2.08
MA−PA/EG	92.8	162.1	169.1	4.31
MA−SA/EG	92.6	174.2	173.1	−0.65
PA−SA/EG	92.8	176.2	179.1	1.65

3.3. Infrared Spectral Analysis of the CPCMs. Fourier transform infrared spectrometry was used to characterize the FABEM PCMs and the FABEM/EG CPCMs, and the FT-IR curves are shown Figure 2. In the spectrograms, the absorption peak of C═O appears at about 1710 cm^{-1} and the bending vibration peak of −CH$_2$− appears at about 1466 cm^{-1}, and the absorption peak in the wavenumber range of about 2925−2854 cm^{-1} overlaps with the C−H stretching vibration absorption peak of the aliphatic group, which is the hydroxyl O−H stretching vibration absorption peak. The above-mentioned data show that the spectral curves of FABEM PCMs and FABEM/EG CPCMs are similar, and the characteristic peaks correspond to each other one by one. It indicates that no new substances are produced in the CPCMs after adding expanded graphite, the structure has not changed, and there is no chemical reaction between the FABEM and EG, and the two are combined together by capillary force and surface tension.

3.4. Microstructure of the CPCMs. The EG and FABEM/EG CPCMs were placed under a scanning electron microscope to observe their micromorphology, and the SEM pictures are shown Figure 3. It can be seen from Figure 3 that EG has a network porous structure formed by the super-position of graphite flakes and a large number of irregular pores, which can make EG better adsorb the FABEM. It can also be seen from Figure 3 that the fatty acid binary eutectic mixtures are evenly adsorbed in the honeycomb-like structure of EG, and leakage does not easily occur. Figure 4 shows the
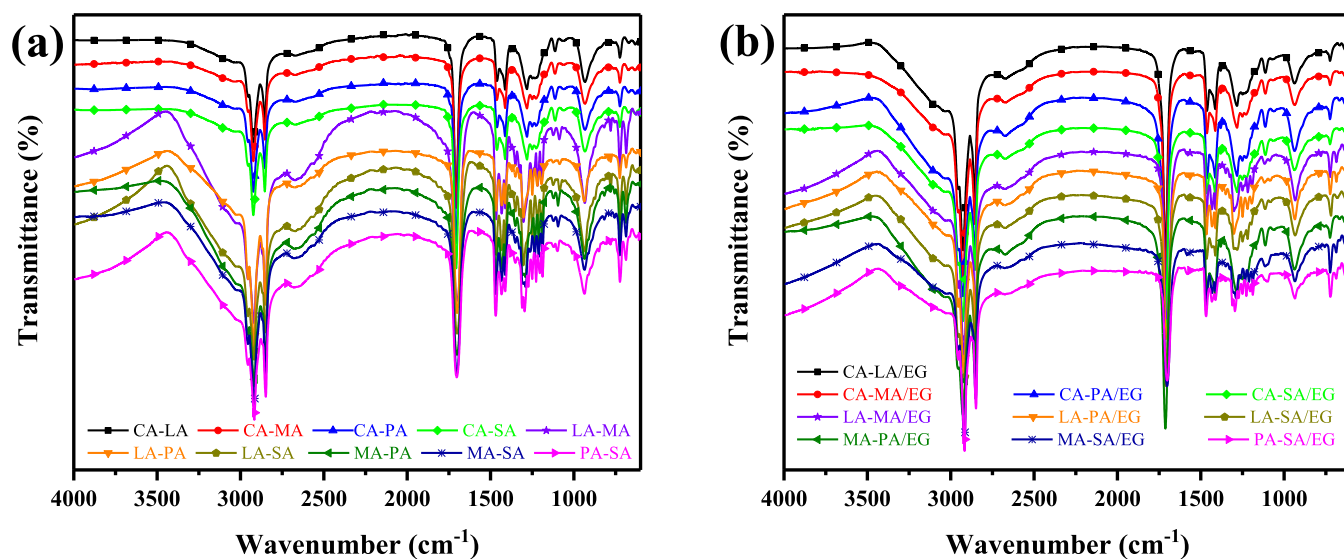
slightly different from that of the CPCM, which is mainly due to the weak interaction between EG and PCMs and the measurement error. The phase change latent heat of CPCMs is lower than that of PCMs and can be calculated by formula 1.

$$H_{mCPCMs} = xH_{mPCMs} \qquad (1)$$

where H_{mCPCMs} is the calculated latent heat of the CPCMs, x is the mass content of PCMs in the CPCMs, H_{mPCMs} is the latent heat of the PCMs. The calculation results and comparison with experimental values are shown in Table 4. The relative errors between the experimental values and the theoretical values are less than ±5%, which shows that the expanded graphite only plays the role of an adsorbent in the CPCMs but not heat storage. These findings demonstrate that these FABEM/EG CPCMs can be used for low-temperature thermal energy storage with appropriate temperature and high phase transition latent heat.

Figure 2. FT-IR curves of 10 fatty acid binary eutectic mixtures (a) and 10 FABEM/EG CPCMs (b).
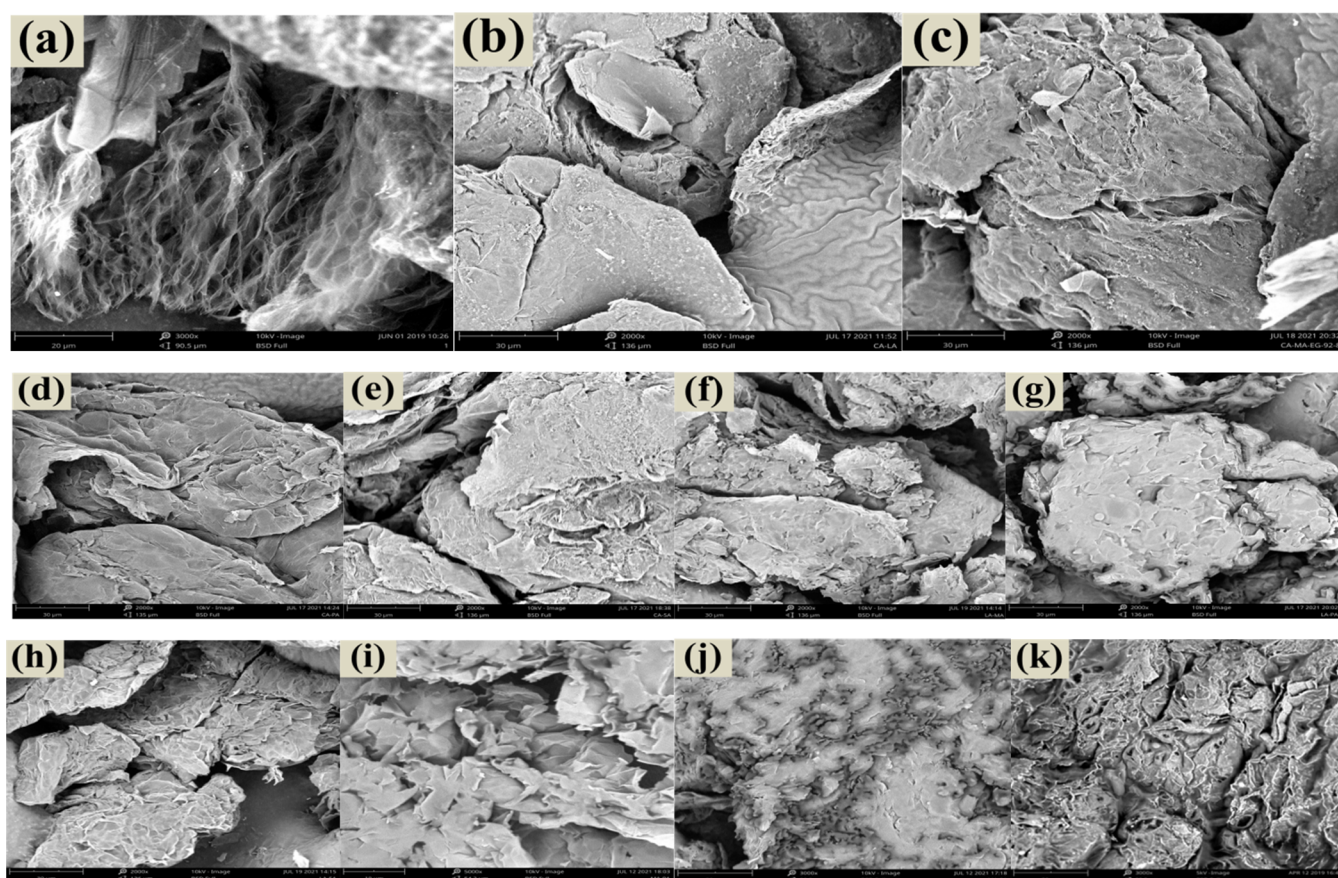

Figure 3. SEM pictures of the 10 FABEM/EG CPCMs and EG. (a) EG, (b) CA−LA/EG, (c) CA−MA/EG, (d) CA−PA/EG, (e) CA−SA/EG, (f) LA−MA/EG, (g) LA−PA/EG, (h) LA−SA/EG, (i) MA−PA/EG, (j) MA−SA/EG, and (k) PA−SA/EG.

microstructure of the CA−LA/EG, CA−MA/EG, and CA−PA/EG after heating and cooling, and there is no leakage in the CPCMs. It shows that the adsorption efficiency of EG toward eutectic mixtures is good, which can prevent the leakage of PCMs and improve the strength of CPCMs.

3.5. Heat Transfer Performance Experiments. The thermal conductivities of CPCMs are significantly improved with the addition of EG. The bulk density of CPCMs

influences their thermal conductivity because of the honeycomb-like structure of EG. The thermal conductivity increases with increasing density. Taking LA−PA/EG CPCMs as an example, the bulk densities are 312.51, 356.46, 392.32, 456.37, 501.67, 557.25, and 603.58 kg/m^3, and the corresponding thermal conductivities are 1.718, 2.358, 2.852, 3.057, 3.564, 4.084, and 4.327 W/(m·K), respectively, as shown in Figure 5. The bulk density and thermal conductivity of LA−PA/EG
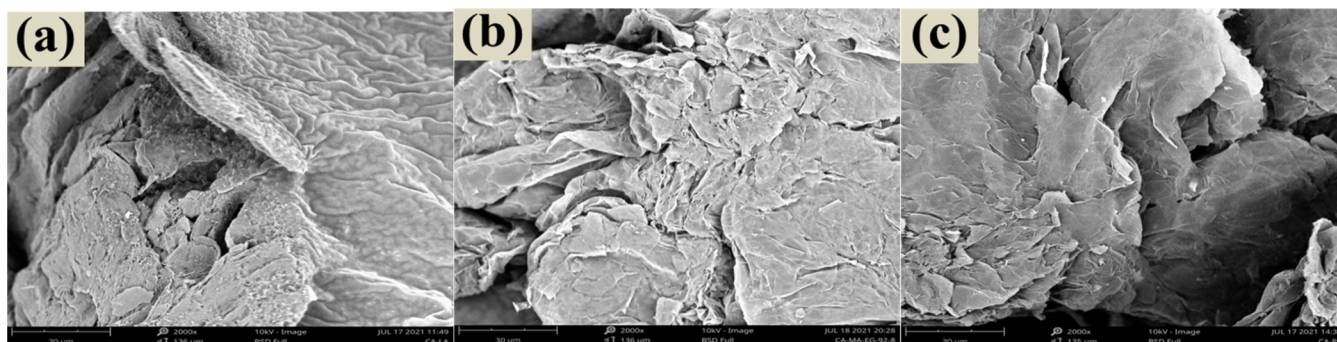
Figure 4. SEM pictures of CPCMs after heating and cooling. (a) CA−LA/EG, (b) CA−MA/EG, and (c) CA−PA/EG.

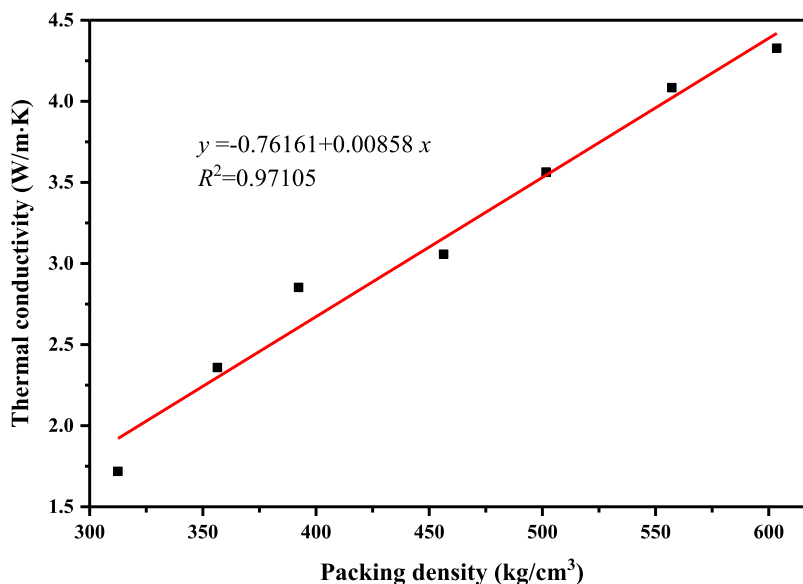$$y = -0.76161 + 0.00858\,x$$
$$R^2 = 0.97105$$

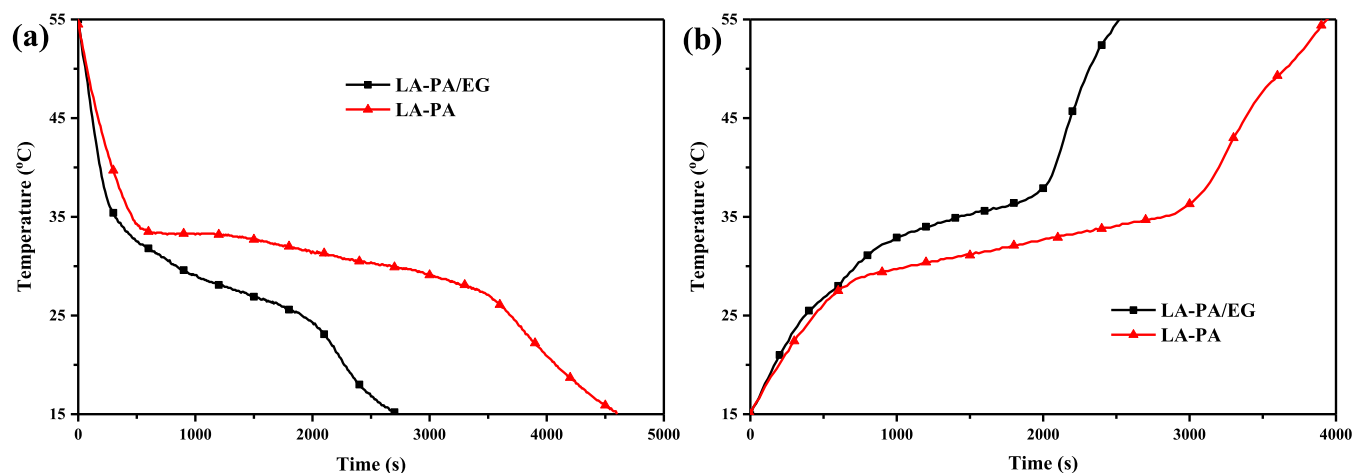**Figure 5.** Thermal conductivity of LA−PA/EG CPCMs varies with packing density.

Figure 6. Solidification (a) and fusion (b) curves of LA−PA and LA−PA/EG.

were found to be linearly related through fitting analysis. The fitting formula is $y = -0.76161 + 0.00858x$ ($R^2 = 0.97105$). The thermal conductivity of LA−PA is about 0.152 W/(m·K). The thermal conductivity of LA−PA/EG CPCM is as high as 2.852 W/(m·K) when the packing density is 392.32 kg/m³, and this value is about 18 times higher than that of LA−PA.

The addition of EG improves the thermal conductivities of CPCMs, which can also be verified from the heat storage and

release test of CPCMs. The same volume of FABEM PCMs and FABEM/EG CPCMs was put into a beaker individually, and the heat storage/release rate was measured by measuring the time when the central temperature of PCMs and CPCMs reaches the set temperature during melting and freezing processes. Taking LA−PA and LA−PA/EG as examples, the volume of the samples after compaction is 60 mL, the bulk density of LA−PA/EG is 392.32 kg/m³, the thermal
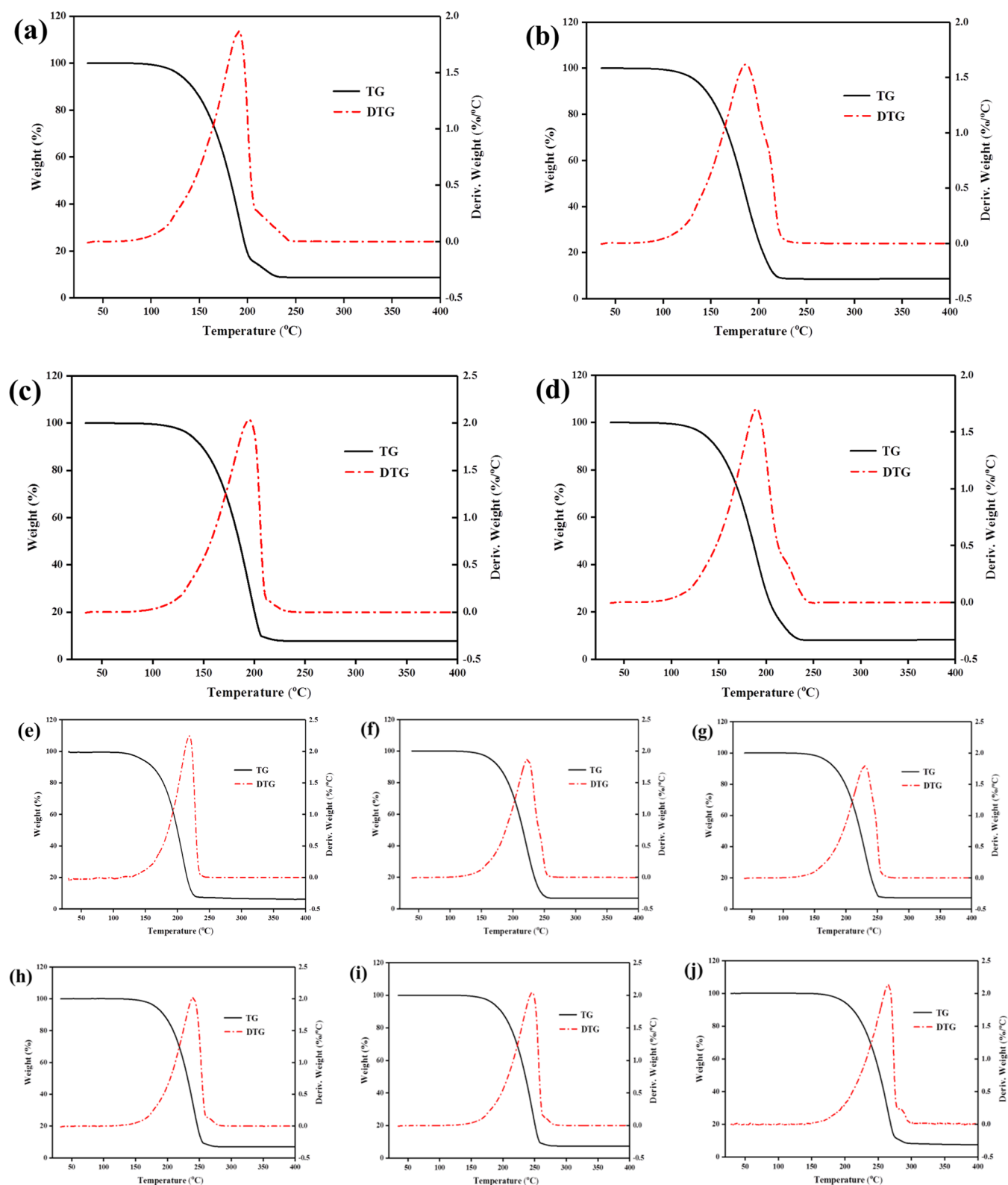
Figure 7. TGA curves of 10 FABEM/EG CPCMs. (a) CA−LA/EG, (b) CA−MA/EG, (c) CA−PA/EG, (d) CA−SA/EG, (e) LA−MA/EG, (f) LA−PA/EG, (g) LA−SA/EG, (h) MA−PA/EG, (i) MA−SA/EG, and (j) PA−SA/EG.

conductivity of LA−PA/EG is 2.852 W/(m·K), and the temperature range is set to 15−55 °C, and the test results are shown in Figure 6. Figure 6a shows the solidification curves of LA−PA and LA−PA/EG, and Figure 6b shows the fusion curves. Figure 6 shows that the LA−PA/EG CPCM achieves the target temperature faster than the LA−PA PCM, suggesting that the thermal conductivity of LA−PA/EG has been greatly improved compared with that of LA−PA. It indicates that the porous structure of EG optimizes the thermal conductivity of the CPCMs.

3.6. Thermostability and Thermoreliability of the CPCMs. The thermostability of the FABEM/EG CPCMs was analyzed by TGA. In a nitrogen environment, the samples were heated from room temperature to 400 °C. Figure 7 and Table 5 show the TGA test results of 10 FABEM/EG CPCMs.

Table 5. Thermal Performance Parameters of 10 Fatty Acid Binary Eutectic Mixtures and 10 FABEM/EG CPCMs

CPCMs	initial weight loss temperature (°C)	epitaxial initiation temperature (°C)	maximum temperature of weight loss rate (°C)
CA−LA/EG	106.2	152.6	191.8
CA−MA/EG	107.4	152.3	184.3
CA−PA/EG	108.6	156.3	191.3
CA−SA/EG	111.3	161.1	194.2
LA−MA/EG	124.1	177.1	219.2
LA−PA/EG	138.8	188.6	225.9
LA−SA/EG	143.5	190.5	232.7
MA−PA/EG	156.1	204.5	242.1
MA−SA/EG	159.5	205.4	247.3
PA−SA/EG	173.6	220.1	265.1

Taking LA−PA as an example, it can be seen from the thermogravimetric curves in Figure 7f and Table 5 that the initial weight loss temperature is about 138.8 °C, suggesting that the LA−PA eutectic mixture progressively starts to evaporate, the epitaxial initiation temperature is 188.6 °C, and the primary weight loss region is between 150 and 230 °C. The maximum temperature of weight loss rate is 225.9 °C. Finally, LA−PA evaporates completely at about 272.5 °C, and the remaining components are expanded graphite and impurities. It can be concluded that 10 CPCMs have good thermal stability in application scenarios at temperature below 100 °C.

Thermoreliability is really a vital function to assess the service life of composite materials. After multiple thermal cycles, the DSC test is performed once more to determine whether the FABEM/EG CPCMs still have adequate thermal reliability. Taking LA−PA/EG CPCMs as an example, the DSC curves are shown in Figure 8. It can be concluded from Figure 8 that after 200 and 1000 thermal cycles, the melting temperature decreased by 0.60 and 1.70 °C, respectively, the melting latent heat reduced by 0.78 and 5.70%, respectively, and the modified values may be disregarded. These results show that these CPCMs have adequate thermal reliability.

4. CONCLUSIONS

The MaxAMR of FABEM PCMs in FABEM/EG CPCMs is 92.0−93.2%, which provides a basis for the preparation of FABEM/EG CPCMs. The phase transition temperatures and latent heat of the FABEM/EG CPCMs are in the range of 17.8−55.2 °C and 134.9−176.2 J/g, respectively. There is only a simple physical adsorption between EG and PCMs and no chemical reaction occurs. The FABEM PCMs are well adsorbed in the pores of EG, and EG can provide a certain mechanical strength and prevent the phase change materials from leaking even when the PCMs are in the molten state. The addition of EG greatly improves the thermal conductivities of CPCMs, which can also be proved by the heat storage/release experiment. The FABEM/EG CPCMs have good thermal stability and excellent thermal cycling reliability in application scenarios at temperature below 100 °C. The above-mentioned results show that the FABEM/EG CPCMs can be used in low-temperature latent heat thermal energy storage systems such as building energy saving, waste heat recovery, and solar energy storage.

■ AUTHOR INFORMATION

Corresponding Author

Dongyi Zhou − *School of Mechanical and Energy Engineering, Shaoyang University, Shaoyang 422000, China; Key Laboratory of Hunan Province for Efficient Power System and Intelligent Manufacturing, Shaoyang University, Shaoyang 422000, China;* orcid.org/0000-0002-8486-8119; Phone: +86-0739-5236-6600; Email: zhoudongyi2005@163.com
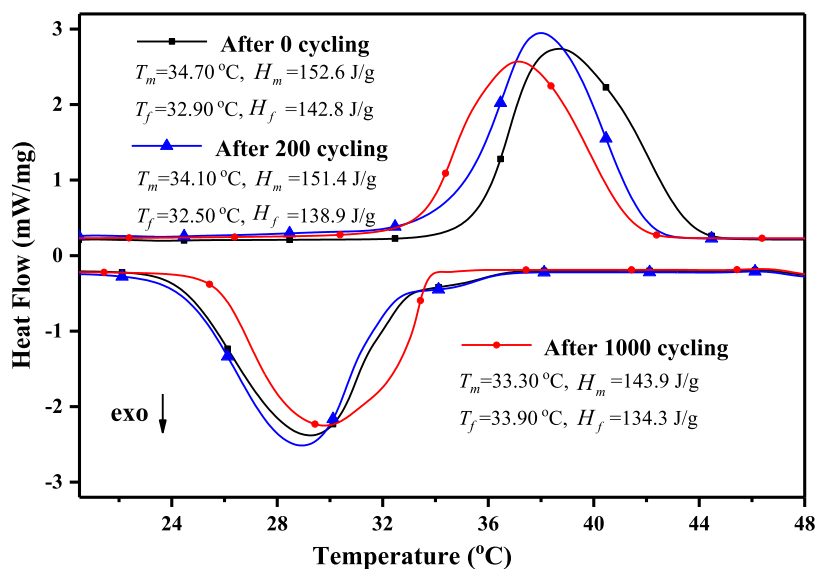

Figure 8. DSC curves of LA−PA/EG CPCMs before and after thermal cycling.

Authors

Shuaizhe Xiao − *School of Mechanical and Energy Engineering, Shaoyang University, Shaoyang 422000, China; Key Laboratory of Hunan Province for Efficient Power System and Intelligent Manufacturing, Shaoyang University, Shaoyang 422000, China*

Xianghua Xiao − *School of Mechanical and Energy Engineering, Shaoyang University, Shaoyang 422000, China; Key Laboratory of Hunan Province for Efficient Power System and Intelligent Manufacturing, Shaoyang University, Shaoyang 422000, China*

Complete contact information is available at:
https://pubs.acs.org/10.1021/acsomega.2c07749

Notes

The authors declare no competing financial interest.

■ REFERENCES

(1) Liu, C.; Song, Y.; Xu, Z.; Zhao, J.; Rao, Z. Highly efficient thermal energy storage enabled by a hierarchical structured hyper-crosslinked polymer/expanded graphite composite. *Int. J. Heat Mass Transfer* **2019**, *148*, No. 119068.

(2) Souayfane, F.; Fardoun, F.; Biwole, P. H. Phase change materials (PCM) for cooling applications in buildings: A review. *Energy Build.* **2016**, *129*, 396−431.

(3) da Cunha, J. P.; Eames, P. Thermal energy storage for low and medium temperature applications using phase change materials -A review. *Appl. Energy* **2016**, *177*, 227−238.

(4) Jamekhorshid, A.; Sadrameli, S. M.; Farid, M. A review of microencapsulation methods of phase change materials (PCMs) as a thermal energy storage (TES) medium. *Renewable Sustainable Energy Rev.* **2014**, *31*, 531−542.

(5) Baskar, I.; Chellapandian, M.; Jaswanth, S. S. H. Development of a novel composite phase change material based paints and mortar for energy storage applications in buildings. *J. Energy Storage* **2022**, *55*, No. 105829.

(6) Jathar, L. D.; Ganesan, S.; Shahapurkar, K.; Soudagar, M. E. M.; Mujtaba, M. A.; Anqi, A. E.; Farooq, M.; Khidmatgar, A.; Goodarzi, M.; Safaei, M. R. Effect of various factors and diverse approaches to enhance the performance of solar stills: a comprehensive review. *J. Therm. Anal. Calorim.* **2022**, *147*, 4491−4522.

(7) Pardo, P.; Deydier, A.; Anxionnaz-Minvielle, Z.; Rouge, S.; Cabassud, M.; Cognet, P. A review on high temperature thermochemical heat energy storage. *Renewable Sustainable Energy Rev.* **2014**, *32*, 591−610.

(8) Aydin, D.; Casey; S, P.; Riffat, S. The latest advancements on thermachemical heat storage systems. *Renewable Sustainable Energy Rev.* **2015**, *41*, 356−367.

(9) Yuan, Y.; Yuan, Y.; Zhang, N.; Du, Y.; Cao, X. Preparation and thermal characterization of capric-myristic-palmitic ac-id/expanded graphite composite as phase change material for energy storage. *Mater. Lett.* **2014**, *125*, 154−157.

(10) Fei, H.; Wang, L.; He, Q.; Du, W.; Gu, Q.; Pan, Y. Preparation and Properties of a Composite Phase Change Energy Storage Gypsum Board Based on Capric Acid-Paraffin/Expanded Graphite. *ACS Omega* **2021**, *6*, 6144−6152.

(11) Liu, C.; Yuan, Y.; Zhang, N.; Cao, X.; Yang, X. A novel PCM of lauric-myristic-stearic acid/expanded graphite composite for thermal energy storage. *Mater. Lett.* **2014**, *120*, 43−46.

(12) Horibe, A.; Jang, H.; Haruki, N.; Sano, Y.; Kanbara, H.; Takahashi, K. Melting and solidification heat transfer characteristics of phase change material in a latent heat storage vessel: Effect of perforated partition plate. *Int. J. Heat Mass Transfer* **2015**, *82*, 259−266.

(13) Liu, F.; Zhu, J.; Liu, J.; Ma, B.; Zhou, W.; Li, R. Preparation and properties of capric-stearic acid/White Carbon Black composite for thermal storage in building envelope. *Energy Build.* **2018**, *158*, 1781−1789.

(14) Elarem, R.; Alqahtani, T.; Mellouli, S.; Aich, W.; et al. Numerical study of an Evacuated Tube Solar Collector incorporating a Nano-PCM as a latent heat storage system. *Case Stud. Therm. Eng.* **2021**, *24*, No. 100859.

(15) Aydin, D.; Casey, S.; Riffat, S. The latest advancements on thermochemical heat storage systems. *Renewable Sustainable Energy Rev.* **2015**, *41*, 356−367.

(16) Sarafraz, M. M.; Safaei, M. R.; Leon, A. S.; Tlili, I.; Alkanhal, T. A.; Tian, Z.; Goodarzi, M.; Arjomandi, M. Experimental Investigation on Thermal Performance of a PV/T-PCM (Photovoltaic/Thermal) System Cooling with a PCM and Nanofluid. *Energies* **2019**, *12*, 2572.

(17) Sun, N.; Xiao, Z. Synthesis and performances of phase change materials microcapsules with a polymer/BN/TiO2 hybrid shell for thermal energy storage. *Energy Fuels* **2017**, *31*, 10186−10195.

(18) Nirwan, A.; Kumar, R.; Mondal, B.; Kumar, J.; Bera, A.; Kumar, R. Thermal performance assessment of lauric acid and palmitic acid based multi-transformation phase change material and exfoliated graphite composites. *Energy Sources, Part A* **2020**, *9*, 1−13.

(19) Kant, K.; Shukla, A.; Sharma, A. Ternary mixture of fatty acids as phase change materials for thermal energy storage applications. *Energy Rep.* **2016**, *2*, 274−279.

(20) Jaksic, J.; Ostojic, S.; Micić, D. M.; Vujosevic, Z. T. Thermal properties of 3-hydroxy fatty acids and their binary mixtures as phase change energy storage materials. *Int. J. Energy Res.* **2019**, *2*, 1294−1302.

(21) Singh, P.; Sharma, R. K.; AnSu, A. K.; Goyal, R.; Sari, A.; Tyagi, V. V. A comprehensive review on development of eutectic organic phase change materials and their composites for low and medium range thermal energy storage applications. *Sol. Energy Mater. Sol. Cells* **2021**, *223*, No. 110955.

(22) Li, T.; Yuan, Y.; Zhang, N. Thermal properties of phase change cement board with capric acid/expanded perlite form-stable phase change material. *Adv. Mech. Eng.* **2017**, *9*, No. 168781401770170.

(23) Zhou, D.; Yuan, J.; Zhou, Y.; Liu, Y. Preparation and Properties of Capric-Myristic Acid/Expanded Graphite Composite Phase Change Materials for Latent Heat Thermal Energy Storage. *Energies* **2020**, *13*, 2462.

(24) Li, C.; Xie, B.; Chen, J. Graphene-decorated silica stabilized stearic acid as a thermal energy storage material. *RSC Adv.* **2017**, *7*, 30142−30151.

(25) Peng, K.; Fu, L.; Li, X.; Ouyang, J.; Yang, H. Stearic acid modified montmorillonite as emerging microcapsules for thermal energy storage. *Appl. Clay Sci.* **2017**, *138*, 100−106.

(26) Safaei, M. R.; Goshayeshi, H. R.; Chaer, I. Solar Still Efficiency Enhancement by Using Graphene Oxide/Paraffin Nano-PCM. *Energies* **2019**, *12*, 2002.

(27) Da Silva, R. S. R.; Oishi, S. S.; Botelho, E. C.; Ferreira, N. G. Carbon foam composites based on expanded graphite for electro-chemical application. *Diamond Relat. Mater.* **2020**, *103*, No. 107730.

(28) McGillicuddy, R. D.; Thapa, S.; Wenny, M. B.; Gonzalez, M. I.; Mason, J. A. Metal-Organic Phase-Change Materials for Thermal Energy Storage. *J. Am. Chem. Soc.* **2020**, *142*, 19170−19180.

(29) Al-Ahmed, A.; Jafar Mazumder, M. A.; Salhi, B.; Sari, A.; Afzaal, M.; Al-Sulaiman, F. A. Effects of carbon-based fillers on thermal properties of fatty acids and their eutectics as phase change materials used for thermal energy storage: A Review. *J. Energy Storage* **2021**, *35*, No. 102329.

(30) Wang, Z.; Huang, G.; Jia, Z.; Gao, Q.; Li, Y.; Gu, Z. Eutectic Fatty Acids Phase Change Materials Improved with Expanded Graphite. *Materials* **2022**, *15*, 6856.

(31) Fei, H.; Du, W.; He, Q.; Gu, Q.; Wang, L. Study of Phase-Transition Characteristics of New Composite Phase Change Materials of Capric Acid-Palmitic Acid/Expanded Graphite. *ACS Omega* **2020**, *5*, 27522−27529.

(32) Huang, X.; Alva, G.; Liu, L.; Fang, G. Preparation, characterization and thermal properties of fatty acid eutectics/bentonite/expanded graphite composites as novel form-stable thermal energy storage materials. *Sol. Energy Mater. Sol. Cells* **2017**, *166*, 157−166.

(33) Sarı, A. Thermal energy storage characteristics of bentonite-based composite PCMs with enhanced thermal conductivity as novel thermal storage building materials. *Energy Convers. Manage.* **2016**, *117*, 132−141.

(34) Zhou, D.; Zhou, Y.; Yuan, J.; Liu, Y. Palmitic Acid-Stearic Acid/Expanded Graphite as Form-Stable Composite Phase-Change Material for Latent Heat Thermal Energy Storage. *J. Nanomater.* **2020**, *2020*, No. 1648080.

(35) Zhou, D.; Yuan, J.; Xiang, H.; Liu, Y. Preparation and Characterization of Lauric-Myristic Acid/Expanded Graphite as Composite Phase Change Energy Storage Material. *J. Nanomater.* **2021**, *2021*, No. 1828147.

(36) Atinafu, D. G.; Dong, W.; Huang, X.; Gao, H.; Wangc, G. Introduction of organic-organic eutectic PCM in mesoporous N-doped carbons for enhanced thermal conductivity and energy storage capacity. *Appl. Energy* **2018**, *211*, 1203−1215.

(37) Zhou, D.; Xiao, S.; Xiao, X.; Liu, Y. Preparation, Phase Diagrams and Characterization of Fatty Acids Binary Eutectic Mixtures for Latent Heat Thermal Energy Storage. *Separations* **2023**, *10*, 49.

(38) Zhou, D.; Xiao, X.; Xiao, B.; Liu, Y. Method of determining optimum mass ratio of fatty acids in composite phase change materials for thermal energy storage. *CIESC J.* **2021**, *72*, 560−566.